ARL-unbiased geometric control charts for high-yield processes

Manuel Cabral Morais (maj@math.ist.utl.pt)

Department of Mathematics & CEMAT — IST, ULisboa, Portugal

IST — Lisboa, October 16, 2019

Quality

- Fitness for use and conformance to requirements are the shortest and most consensual definitions of quality (Juran and Godfrey, 1999, p. 27; Crosby, 1979, p. 17).
- A curious fact that escapes most consumers nowadays: concerns about quality can be traced back to the Babylonian Empire, 1830BC–539BC (Gitlow *et al.*, 1989, pp. 8–9).

  Code of Hammurabi[1]

  Law 229: *If a builder builds a house for a man and does not make its construction firm, and the house which he has built collapse and cause the death of the owner of the house, that builder shall be put to death.*
- This *eye for an eye* approach to quality was also adopted by Phoenicians inspectors, who *eliminated any repeated violations of quality standards by chopping off the hand of the maker of the defective product* (Gitlow *et al.*, 1989, p. 9).

[1] A Babylonian law code, dating back to about 1772BC, named after the sixth Babylonian king, who enacted it. It consists of 282 laws dealing with matters of contracts, terms of transactions or addressing household and family relationships such as inheritance, divorce, paternity and sexual behavior.

The founder of statistical process control (SPC)

- We have to leap to the 20th. century to meet the American physicist, engineer and statistician Walter Andrew Shewhart (1891–1967).

  By proposing a quality control chart to his superiors (Bell Laboratories), in a memorandum on May 16, 1924, Shewhart altered the course of industrial history, brought together statistics, engineering, and economics and became known as the father of modern quality control.

Quality control charts

- Are used to track process performance over time and detect changes in a process parameter, by plotting the observed value of a statistic against time and comparing it with a pair of suitable control limits.

  An obs. beyond the control limits indicate potential assignable causes responsible for changes in that parameter, thus, should be investigated...

- Applications

  Computer intrusion detection, finance, health care, queueing systems, staff management, water monitoring, etc.

Nonconformity; nonconforming item

- Each specification that is not satisfied by a unit of a product is considered a defect or nonconformity (Montgomery, 2009, p. 308).
- A unit with a least one defect is called a defective or nonconforming item.

Examples of high-yield industrial processes

Many processes produce defectives items at a rate less than 100 ppm.

- Wire bonding process in an integrated circuit assembly provides an electrical connection between a semiconductor die and the external leads (Chang and Gan, 2001).
- In the filling process in the manufacture of low voltage liquid crystal display units, an incompletely filled unit is regarded as a nonconforming item (Chan *et al.*, 2003).
- Exhaust valves seats are force fitted by insertion into the head of an engine; incorrect installation can lead to an engine failure; the target defective rate is less than 50 ppm (Steiner *et al.*, 2004).

Geometric chart with 3-σ limits

- The most popular procedure to monitor high-yield industrial processes can be traced back to Calvin (1983).
- **Control statistic**: cumulative count of conforming (CCC) items between the $(t-1)^{th}$ and t^{th} nonconforming units, X_t.
- **Distribution**: $X_t \overset{indep.}{\sim}$ geometric$^*(p)$; $P_p(x) = (1-p)^x\, p,\ x \in \mathbb{N}_0$.
- **Parameter**: p (fraction nonconforming).
- **Target value of p**: p_0.
- **True value of p**: $\rho \times p_0$ $(0 < \rho < 1/p_0;\ \rho$ magnitude of the shift).
- $3-\sigma$ **control limits**:

$$LCL = (1-p_0)/p_0 - 3\sqrt{\frac{1-p_0}{p_0^2}}; \quad UCL = (1-p_0)/p_0 + 3\sqrt{\frac{1-p_0}{p_0^2}}.$$

- Triggers a signal and we **deem the process** (mean) **out-of-control** if $X_t \notin [LCL, UCL]$.
- Plot the number of conforming units (between consecutive conforming units) on a **logarithmic scale** to accommodate large values of X_t.

Example 1

- Wire bonding process in an integrated circuit
  $p_0 = 10^{-4}$ (target fraction nonconforming)
- Simulated data: first 50 obs. of X_t — process in-control; last 20 obs. of X_t — process out-of-control ($p = 2 \times p_0$).
- $LCL = \left\lceil \max\left\{0,\ (1-p_0)/p_0 - 3\sqrt{(1-p_0)/p_0^2}\right\} \right\rceil = 0$

  $UCL = \left\lfloor (1-p_0)/p_0 + 3\sqrt{(1-p_0)/p_0^2} \right\rfloor = 39\,997.$
- Geometric chart

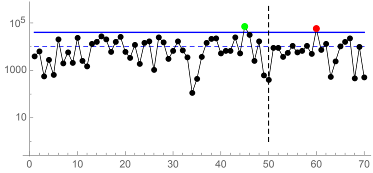

One false alarm: unit $506\,313 + 45$ $(x_{45} = 70\,728)$

One valid signal: unit $678\,446 + (50 + 10)$ $(x_{60} = 55\,600)$

Performance of geometric charts

- **Run length** (RL) — number of conforming units we collect until a signal is triggered by the geometric chart with control limits L and U.

$$\begin{aligned} RL(\rho) &\sim \text{geometric}\,(\xi(\rho) = P(signal \mid p = \rho\, p_0)) \\ \xi(\rho) &= P_{\rho\, p_0}(X \notin [L, U]) = 1 - \textstyle\sum_{x=L}^{U} P_{\rho\, p_0}(x) \\ P[RL(\rho) = y] &= [1 - \xi(\rho)]^{y-1}\, \xi(\rho),\ y \in \mathbb{N} \\ ARL(\rho) &= 1/\xi(\rho) \qquad \textbf{average run length}. \end{aligned}$$

  It is desirable that valid signals/false alarms are emitted as quickly/rarely as possible, corresponding to small out-of-control/large in-control **ARL**.

- It is crucial to swiftly detect not only increases but also decreases in p.

  Increases in p mean process deterioration.

  Decreases in p represent process improvement (to be noted and possibly incorporated). It can also mean that a new inspector may not have been trained properly to inspect the process output.

Performance of geometric charts (cont'd)

- Ideally, the **ARL function should achieve a maximum when the process is in-control** (the chart takes longer, in average, to trigger a false alarm than to detect any shifts), i.e., the chart is **ARL-unbiased**

  (Pignatiello *et al.*, 1995; Basseville and Nikiforov, 1993).

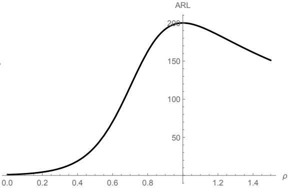

Disadvantages of geometric charts

- Keep in mind that $\left\lceil \max\left\{0, (1-p_0)/p_0 - 3\sqrt{(1-p_0)/p_0^2}\right\}\right\rceil = 0$ means $ARL(\rho) > ARL(1)$, for $\rho > 1$, i.e., the chart triggers false alarms more frequently than valid signals in the presence of increases in p.

- ARL-biased!

  Inability to have a pre-specified in-control ARL, $ARL^\star$, when the control statistic is a discrete r.v. (c.d.f. is a step function).

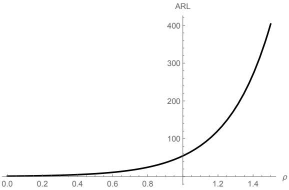

Variants to mitigate the poor performance of the geometric chart

- Xie and Goh (1997) recommended the use of *exact probability limits*:

$$LCL_\alpha = \ln(1-\alpha/2)/\ln(1-p_0), \quad \text{and} \quad UCL_\alpha = \ln(\alpha/2)/\ln(1-p_0),$$

  where $\alpha = 1/ARL^\star$ represents the acceptable risk of false alarm.

- Zhang *et al.* (2004) suggested:
  - taking $L \in A = \{1, \ldots, LCL_{max}\}$, with $LCL_{max} = \lfloor \ln(1-\alpha)/\ln(1-p_0) \rfloor$;
  - finding $U : P_{\rho p_0}(X < L) + P_{\rho p_0}(X > U) \approx \alpha$, for each $L \in A$;
  - defining the set C of all such pairs of control limits (L, U);
  - choosing $(L^*, U^*) \in C$ that *most nearly equalizes the tail probab.*, i.e.,

$$|P_{p_0}(X < L^*) - P_{p_0}(X > U^*)| = \min_{(L,U)\in C} |P_{p_0}(X < L) - P_{p_0}(X > U)|.$$

$$ARL^*(\rho) = [P_{\rho\, p_0}(X < L^*) + P_{\rho\, p_0}(X > U^*)]^{-1}, \quad 0 < \rho < 1/p_0.$$

Both charts are ARL-biased: ARL does not attain a maximum at $\rho = 1$.
Moreover, the in-control ARL does not coincide with $ARL^\star$, a pre-chosen value.

Yet Zhang *et al.* (2004) calls it a *nearly ARL-unbiased geometric chart.*

- Inspired by **UMPU** and **randomized** tests [2] (rarely used in SPC), we defined a **geometric chart that triggers a signal** with:
  - **probability one** if the obs. number of conforming units between two consecutive nonconforming units, x, **is below L or above U**;
  - **probability** γ_L (resp. γ_U) if $x = L$ (resp. $x = U$).
- A signal is triggered by this chart with probability

$$\xi_{unb}(\rho) = 1 - \sum_{x=L}^{U} P_{\rho\, p_0}(x) + \gamma_L \times P_{\rho\, p_0}(L) + \gamma_U \times P_{\rho\, p_0}(U).$$

Its corresponding ARL function: $ARL_{unb}(\rho) = 1/\xi_{unb}(\rho)$.

- The **randomization probabilities** and the new **control limits** satisfy:

$$ARL_{unb}(1) = ARL^{\star}; \qquad \left.\frac{dARL_{unb}(\rho)}{d\rho}\right|_{\rho=1} = 0.$$

These two equations are not sufficient to define a pair of control limits (L, U) and a pair of randomization probabilities (γ_L, γ_U).

Way out...

[2] UMPU, uniformly most powerful unbiased (Lehmann, 1959, pp. 125–130; see Appendix 1).

- Consider

$$\gamma_L = \frac{d\,e - b\,f}{a\,d - b\,c}, \qquad \gamma_U = \frac{a\,f - c\,e}{a\,d - b\,c},$$

where: $\quad a = P_{p_0}(L), \quad b = P_{p_0}(U), \quad c = L \times P_{p_0}(L), \quad d = U \times\ P_{p_0}(U),$

$$e = \frac{1}{ARL^\star} - 1 + \sum_{x=L}^{U} P_{p_0}(x), \quad f = \frac{1}{ARL^\star} \times E_{p_0}(X) - E_{p_0}(X) + \sum_{x=L}^{U} x \times P_{p_0}(x).$$

- To rule out control limits leading to $(\gamma_L, \gamma_U) \notin (0,1)^2$, (L, U) is restricted to the following *suitable* grid (see Appendix 2) of non-negative integer numbers:

$$\{(L,U) : \; L_{min} \leq L \leq L_{max}, \; U_{min} \leq U \leq U_{max}\}.$$

- **Randomization of the emission of the signal**

  Can be done in practice by incorporating the generation of a pseudo-random number from a Bernoulli distribution with parameter γ_L (resp. γ_L) in the software used to monitor the data fed from the production line, whenever the observed control statistic is equal to LCL (resp. U).

Example 2 — ARL-unbiased geometric charts

- $p_0 = 10^{-i}$, $i = 5, 4, 3, 2$
- $ARL^\star = 200, 370.4 \quad (\alpha = 0.005, 0.0027)$
- Limits of the search grid, control limits and randomization probabilities

	$ARL^\star = 200$							
p_0	L_{min}	L_{max}	L	U_{min}	U_{max}	U	γ_L	γ_U
0.00001	441	501	441	743009	743294	743230	0.792137	0.754626
0.0001	44	50	44	74298	74326	74319	0.177234	0.318435
0.001	4	5	4	7426	7430	7428	0.415872	0.349557
0.01	0	0	0	739	739	739	0.440987	0.207035
	$ARL^\star = 370.4$							
p_0	L_{min}	L_{max}	L	U_{min}	U_{max}	U	γ_L	γ_U
0.00001	240	270	240	812554	812706	812674	0.736799	0.103324
0.0001	24	27	24	81252	81267	81263	0.072600	0.166090
0.001	2	2	2	8122	8123	8122	0.406312	0.224264
0.01	0	0	0	808	808	808	0.240561	0.010422

Expectedly, the search grid/control limits grow comparatively larger, as we deal with smaller values of the target fraction nonconforming.

Example 3 — *Nearly ARL-unbiased* vs. ARL-unbiased geometric charts

- $p_0 = 10^{-3}$, $ARL^\star = 200$
- Relative gain in the ARL when we replace the *nearly* ARL-unbiased design by the ARL-unbiased chart: $[1 - ARL(\rho,\gamma_L,\gamma_U)/ARL^*(\rho)] \times 100\%$.

	$ARL(\rho)$		
ρ	*nearly* unbiased	unbiased	% gain
0.5	29.6309	37.6573	−27.0878%
0.8	138.8971	162.7097	−17.1440%
0.9	178.4955	191.8332	−7.4723%
1.0	199.9869	200.0000	−0.0066%
1.1	204.1971	194.9502	4.5285%
1.2	198.2454	184.4424	6.9626%
1.5	166.1584	151.0359	9.1013%

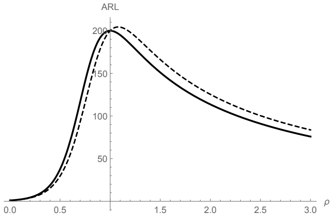

- The randomization of the emission of a signal allows the ARL-unbiased geometric chart to take less time to detect decreases in p than to trigger a false alarm, even if we are dealing with a null LCL.
- The out-of-control ARL performance of the *nearly ARL unbiased* and the ARL-unbiased geometric charts differ markedly when $p_0 \geq 10^{-3}$.
- The ARL-unbiased geometric chart is more (resp. less) sensitive to proc. deterioration (resp. improvement) than the *nearly ARL-unbiased* geom. chart.

- **ARL-unbiased geometric chart**

  As opposed to the geometric chart with 3-σ limits and its variants...

  - The ARL-unbiased geometric chart can take a **pre-specified in-control ARL** and the associated **ARL curve attain a maximum when p is on target**.
  - It **tackles the curse of the null LCL** and has the potential to play a major role in the timely detection of the deterioration and improvement of real high-yield processes.

- **Future work**

  - ARL-unbiased versions of the existing $CCC - r$ charts to monitor the cumulative count of conforming items until the r^{th} nonconforming item,[3] suchlike the ones discussed by Xie *et al.* (1998), ..., Albers (2010).
  - ARL-unbiased designs of the CUSUM (cumulative sum) and EWMA (exponentially weighted moving average) charts proposed by Chang and Gan (2001) and Yeh *et al.* (2008) for geometric output.

[3] X has a negative binomial distribution with parameters r and p.

UMP and UMPU tests

- A size $\alpha = (ARL^\star)^{-1}$ test for $H_0 : p = p_0$ against $H_1 : p = \rho\, p_0 \neq p_0$, with power function $\xi(\rho)$, is said to be **unbiased** if $\xi(0) \leq (ARL^\star)^{-1}$ and $\xi(\rho) \geq (ARL^\star)^{-1}$, for $\rho \neq 1$.

  The test is at least as likely to reject under any alternative as under H_0;

$$ARL(1) \geq ARL^\star \qquad \text{and} \qquad ARL(\rho) \leq ARL^\star,\ \rho \neq 1.$$

- If we consider $\mathcal{C}$ a class of tests for $H_0 : \mu = \mu_0$ against $H_1 : p \neq p_0$, then a test in $\mathcal{C}$, with power function $\xi(\rho)$, is a **uniformly most powerful (UMP)** class $\mathcal{C}$ **test** if $\xi(\rho) \geq \xi'(\rho)$, for every $\rho \neq 1$ and every $\xi'(\rho)$ that is a power function of a test in class $\mathcal{C}$.

- In this situation there is no UMP test, but there is a test which is UMP among the class of all unbiased tests — the **uniformly most powerful unbiased (UMPU) test**.

- The concept of an **ARL-unbiased** Shewhart-type **chart** is related to the notion of **UMPU test**.

UMPU tests in the geometric case

- The UMPU test derived by Lehmann (1986, pp. 135–136) for a real-valued parameter p of a distribution in the exponential family (such as the geometric distribution) uses the critical function

$$\phi(x) = P(\text{Reject } H_0 \mid X = x) = \begin{cases} 1 & \text{if } x < L \text{ or } x > U \\ \gamma_L & \text{if } x = L \\ \gamma_U & \text{if } x = U \\ 0 & \text{if } L < x < U, \end{cases}$$

where L, U, γ_L, and γ_U are such that:

$$\begin{aligned} E_{p_0}[\phi(X)] &= (ARL^\star)^{-1} && \text{(prob. of false alarm} = (ARL^\star)^{-1}); \\ E_{p_0}[X\,\phi(X)] &= (ARL^\star)^{-1} \times E_{p_0}(X) && \text{(unbiased ARL).} \end{aligned}$$

- These equations are equivalent to

$$\begin{aligned} \gamma_L \times P_{p_0}(L) &+ \gamma_U \times P_{p_0}(U) = (ARL^\star)^{-1} - \left[1 - \sum\nolimits_{x=L}^{U} P_{p_0}(x)\right] \\ \gamma_L \times L \times P_{p_0}(L) &+ \gamma_U \times U \times P_{p_0}(U) \\ &= (ARL^\star)^{-1} \times E_{p_0}(X) - \left[E_{p_0}(X) - \sum\nolimits_{x=L}^{U} x \times P_{p_0}(x)\right]. \quad (2) \end{aligned}$$

- (1)–(2) are not sufficient to define L, U, γ_L, γ_U.

- Searching for (L, U) and (γ_L, γ_U)

Let $\alpha = (ARL^\star)^{-1}$ be the desired probability of false alarm.

The search for admissible values for (γ_L, γ_U) starts with $(L, U) = (L_{min}, U_{min})$ and stops as soon as an admissible solution is found.

Suitable search grid: $\{(L, U) : L_{min} \leq L \leq L_{max},\ U_{min} \leq U \leq U_{max}\}$, where

- $L_{min} = \max\left\{F^{-1}\left(\max\{0,\ F(U_{min}-1) - 1 + \alpha\}\right),\ G^{-1}\left(\max\{0,\ G(U_{min}-1) - 1 + \alpha\}\right)\right\}$
- $L_{max} = \min\left\{\tilde{F}^{-1}(\alpha),\ \tilde{G}^{-1}(\alpha)\right\}$
- $U_{min} = \max\left\{F^{-1}(1-\alpha),\ G^{-1}(1-\alpha)\right\}$
- $U_{max} = \min\left\{\tilde{F}^{-1}\left(\min\{1,\ F(L_{max}) + 1 - \alpha\}\right),\ \tilde{G}^{-1}\left(\min\{1,\ G(L_{max}) + 1 - \alpha\}\right)\right\}$
- $F(x) = P_{p_0}(X \leq x)$ $\quad G(x) = \frac{1}{E_{p_0}(X)} \sum_{i=0}^{x} i \times P_{p_0}(X = i)$
- $F^{-1}(\alpha) = \min\{x \in \mathbb{N}_0 : F(x) \geq \alpha\}$ $\quad \tilde{F}^{-1}(\alpha) = \min\{x \in \mathbb{N}_0 : F(x) > \alpha\}$
- $G^{-1}(\alpha) = \min\{x \in \mathbb{N}_0 : G(x) \geq \alpha\}$ $\quad \tilde{G}^{-1}(\alpha) = \min\{x \in \mathbb{N}_0 : G(x) > \alpha\}$.

Rationale (Paulino *et al.*, 2016a, Appendix C)

Setting $\gamma_L = \gamma_U = 0$ (resp. $\gamma_L = \gamma_U = 1$) in eq. (1) and (2) leads to:

$\alpha \geq F(L-1) + 1 - F(U)$ and $\alpha \geq G(L-1) + 1 - G(U)$;

(resp. $\alpha \leq F(L) + 1 - F(U-1)$ and $\alpha \leq G(L) + 1 - G(U-1)$).

- Acosta-Mejía, C. A. (1999). Improved p-charts to Monitor Process Quality, *IIE Transactions* 31: 509–516.
- Albers, W. (2010). The Optimal Choice of Negative Binomial Charts for Monitoring High-quality Processes, *Journal of Statistical Planning and Inference* 140: 214–225.
- Basseville, M. and Nikiforov, I.V. (1993). *Detection of Abrupt Changes: Theory and Application*. Prentice-Hall.
- Bourke, P. D. (2001). The Geometric CUSUM Chart with Sampling Inspection for Monitoring Fraction Defective, *Journal of Applied Statistics* 28: 951–972.
- Calvin, T. W. (1983). Quality Control Techniques for 'Zero-defects', *IEEE Transactions on Components, Hybrids, and Manufacturing Technology*, CHMT-6: 323–28.
- Chan, L. Y., Lai, C. D., Xie, M., and Goh, T. N. (2003). A Two-stage Decision Procedure for Monitoring Processes with Low Fraction Nonconforming, *European Journal of Operational Research* 150: 420–436.
- Chan, L. Y. and Wu, S. (2009). Optimal Design for Inspection and Maintenance Policy Based on the CCC Chart, *Computers & Industrial Engineering* 57: 667–676.
- Chang, T. C. and Gan, F. F. (2001). Cumulative Sum Charts for High Yield Processes, *Statistica Sinica* 11: 791–805.
- Chen, J. T. (2009). A New Approach to Setting Control Limits of Cumulative Count of Conforming Charts for High-yield Processes, *Quality and Reliability Engineering International* 25: 973–986.
- Cox, D. R. and Hinkley, D. V. (1974). *Theoretical Statistics*, London: Chapman and Hall.
- Geyer, C.J. and Meeden, G.D. (2004). ump: An R package for UMP and UMPU tests. Available at `www.stat.umn.edu/geyer/fuzz/`
- Geyer, C.J. and Meeden, G.D. (2005). Fuzzy and randomized confidence intervals and p-values. *Statistical Science* **20**, 358–366.
- Glushkovsky, E. A. (1994). On-line-G-control Chart for Attribute Data, *Quality and Reliability Engineering International* 10: 217–227.
- Goh, T. N. (1987). A Control Chart for Very High Yield Processes, *Quality Assurance* 13: 18–22.
- Guo, B., Wang, B. X., and Xie, M. (2014). ARL-unbiased Control Charts for the Monitoring of Exponentially Distributed Characteristics Based on Type-II Censored Samples, *Journal of Statistical Computation and Simulation* 84: 2734–2747.

- Guo, B. and Wang, B. X. (2015). The Design of the ARL-unbiased S^2 Chart when the In-control Variance is Estimated, *Quality and Reliability Engineering International* 31: 501–511.
- Kaminsky, F. C., Benneyan, J. C., Davis, R. D., and Burke, R. J. (1992). Statistical Control Charts Based on a Geometric Distribution, *Journal of Quality Technology* 24: 63–69.
- Knoth, S. and Morais, M. C. (2013). On ARL-unbiased control charts, in *Proceedings XIth. International Workshop on Intelligent Statistical Quality Control*, August 20–23, 2013, pp. 31–50, Sydney, Australia.
- Knoth, S., and Morais, M. C. (2015). On ARL-unbiased control charts, in *Frontiers in Statistical Quality Control, Vol. 11*, S. Knoth and W. Schmid, eds., pp. 95–117, Switzerland: Springer International Publishing.
- Kuralmani, V., Xie, M. and Gan, F. F. (2002). A Conditional Decision Procedure for High Yield Processes., *IIE Transactions* 34: 1021–1030.
- Lehmann, E.L. (1959). *Testing Statistical Hypotheses*. John Wiley & Sons.
- Li, Z., Qiu, P., Chatterjee, S., and Wang, Z. (2013). Using p Values to Design Statistical Process Control Charts, *Statistical Papers* 54: 523–539.
- Liu, J. Y., Xie, M., Goh, T. N., Liu, Q. H., and Zhang, Z. H. (2006). Cumulative Count of Conforming Chart with Variable Sampling Intervals, *International Journal of Production Economics* 101: 286–297.
- Morais, M. C. (2016). An ARL-unbiased np-chart, *Economic Quality Control* 31: 11–21.
- Morais, M. C. (2017). ARL-unbiased geometric and CCC_G control charts, *Sequential Analysis* 36: 513–527.
- Nelson, L. S. (1994). A Control Chart for Parts-per-million Nonconforming Items, *Journal of Quality Techonology* 26: 239–240.
- Ohta, H., Kusukawa, E., and Rahim, A. (2001). A CCC-r Chart for High-yield Processes, *Quality and Reliability Engineering International* 17: 439–446.
- Paulino, S., Morais, M. C., and Knoth, S. (2016a). An ARL-unbiased c-chart, *Quality and Reliability Engineering International*, 32: 2847–2858.

- Paulino, S., Morais, M. C., and Knoth, S. (2016b). On ARL-unbiased c-charts for INAR(1) Poisson Counts. *Statistical Papers*. http://rdcu.be/nGs8.
- Pignatiello, J. J. Jr., Acosta-Mejía, C. A., and Rao, B. V. (1995). The Performance of Control Charts for Monitoring Process Dispersion, in *4th Industrial Engineering Research Conference Proceedings* 24–25 May, 1995, pp. 320–328, Nashville, Tennessee, USA.
- Quesenberry, C. P. (1995). Geometric Q Charts for High Quality Processes (with discussion), *Journal of Quality Technology* 27: 304–343.
- R Core Team (2013). R: A Language and Environment for Statistical Computing, R Foundation for Statistical Computing. Vienna, Austria. http://www.R-project.org/.
- Schwertman, N. C. (2005). Designing Accurate Control Charts Based on the Geometric and Negative Binomial Distributions, *Quality and Reliability Engineering International* 21: 743–756.
- Shao, J. (2005). *Mathematical Statistics: Exercises and Solutions*, New York, NY: Springer Science+Business Media, Inc.
- Steiner, S. H. and MacKay, R. J. (2004). Effective monitoring of processes with parts per million defective. A hard problem!, in *Frontiers in Statistical Quality Control, Vol. 7*, H.-J. Lenz and P.-T. Wilrich, eds., pp. 140–149, Heidelberg: Physica-Verlag.
- Tang, L. C. and Cheong, W. T. (2004). Cumulative Conformance Count Chart with Sequentially Updated Parameters, *IIE Transactions* 36: 841–853.
- Tang, L. C. and Cheong, W. T. (2006). A Control Scheme for High-yield Correlated Production under Group Inspection, *Journal of Quality Technology* 16: 45–55.
- Wolfram Research, Inc. (2015). *Mathematica (Version 10.3) [Computer software]*. Champaign, IL.
- Wu, Z., Yeo, S. H., and Fan, H. (2000). A comparative study of the CRL-type control charts, *Quality and Reliability Engineering International* 16: 269–279.
- Wu, Z., Zhang, X., and Yeo, S. H. (2001). Design of the Sum-of-conforming-run-length Control Charts, *European Journal of Operational Research* 132: 187–196.
- Xie, M. and Goh, T. N. (1997). The Use of Probability Limits for Process Control Based on Geometric Distributions, *International Journal of Quality and Reliability Management* 14: 64–73.

- Xie, M., Goh, T. N., and Kuralmani, V. (2000). On Optimal Setting of Control Limits for Geometric Chart, *International Journal of Reliability, Quality and Safety Engineering* 7: 17–25.
- Xie, M., Goh, T. N., and Lu, X. S. (1998). A Comparative Study of CCC and CUSUM Charts, *Quality and Reliability Engineering International* 14, 339–345.
- Yang, Z., Xie, M., Kuralmani, V., and Tsui, K. L. (2002). On the Performance of Geometric Chart with Estimated Control Limits, *Journal of Quality Technology* 34: 448–458.
- Yeh, A. B., McGrath, R. N., Sembower, M. A., and Shen, Q. (2008). EWMA Control Charts for Monitoring High-yield Processes Based on Non-transformed Observations, *International Journal of Production Research* 46: 5679–5699.
- Zhang, L., Govindaraju, K., Bebbington, M. and Lai, C. D. (2004). On the Statistical Design of Geometric Control Charts, *Quality Technology & Quantitative Management* 2: 233–243.
- Zhang, M., Peng, Y., Schuh, A., Megahed, F. M., and Woodall, W. H. (2012). Geometric Charts with Estimated Control Limits, *Quality and Reliability Engineering International* 29: 209–223.
- Zhang, C. W., Xie, M., and Goh, T. N. (2006). Design of Exponential Control Charts Using a Sequential Sampling Scheme, *IIE Transactions* 38: 1105–1116.
- Zhang, C. W., Xie, M., and Goh, T. N. (2008). Economic Design of Cumulative Conforming Control Chart under Sampling Inspection, *International Journal of Production Research* 38: 1105–1116.
- Zhang, C. W., Xie, M., and Jin, T. (2012). An Improved Self-starting Cumulative Count of Conforming Chart for Monitoring High-quality Processes under Group Inspection, *International Journal of Production Research* 50: 7026–7043.